PCCP

PAPER

View Article Online
View Journal | View Issue

Cite this: *Phys. Chem. Chem. Phys.*, 2015, **17**, 20515

Strong electron donation induced differential nonradiative decay pathways for *para* and *meta* GFP chromophore analogues†

Tanmay Chatterjee, Mrinal Mandal, Venkatesh Gude, Partha Pratim Bag and Prasun K. Mandal*

Received 28th May 2015,
Accepted 22nd June 2015

DOI: 10.1039/c5cp03086b

www.rsc.org/pccp

Z–E Isomerisation because of rotation around the exocyclic double bond (known as the τ-twist) and not any other internal conversion has been reported to be the major nonradiative decay channel for non-hydroxylic unconstrained *para* and *meta* GFP chromophore analogues. The equation $\Phi_f + 2\Phi_{ZE} = 1$ has been shown to hold well for both *para* and *meta* GFP chromophore analogues. If the above equation holds true, then upon reducing the extent of *Z–E* isomerisation (Φ_{ZE}), the fluorescence quantum yield (Φ_f) should increase. To probe the above proposition two sets of non-hydroxylic unconstrained *para* and *meta* GFP chromophore analogues were synthesized. Quite interestingly by introducing the strongly electron donating $-NEt_2$ group to the benzenic moiety these *para* and *meta* GFP chromophore analogues were shown to exhibit differential optical behaviour w.r.t. the extent of the solvatochromic shift, Φ_f, Φ_{ZE}, and τ_f. For the first time it has been shown that the well accepted equation $\Phi_f + 2\Phi_{ZE} = 1$ does not hold at all for these non-hydroxylic unconstrained *meta* analogues. Although Φ_{ZE} has been shown to be <10%, Φ_f is much lower than the expected near unity value for these *meta* analogues. After detailed investigation into the nonradiative excited state decay channel, contrary to literature reports, energy gap law governed internal conversion and not *Z–E* isomerisation was shown to be the major nonradiative decay channel for these *meta* analogues. Two models are put forward to understand the differential optical behaviour of these *para* and *meta* GFP chromophore analogues. Support from X-ray crystal structures, NMR experiments, and computational calculations has also been provided.

Introduction

Z–E Isomerisation because of rotation around the exocyclic double bond (τ-twist, see Chart 1), and not any other internal conversion has been reported to be the major nonradiative decay channel, because of which the fluorescence quantum yield (Φ_f) of the GFP chromophore (*p*-HBDI, see Chart 1) in normal solvents is reduced.[1–8] This proposition has been extended to other unconstrained GFP chromophore analogues.[9–12] For example both *p*-HBDI and *p*-ABDI (Chart 1) have a *Z–E* isomerisation quantum yield (Φ_{ZE}) $\sim$ 0.5 and $\Phi_f \sim$ 0.0001.[9] However, *meta* analogues of these two molecules *i.e.* *m*-HBDI and *m*-ABDI possess a Φ_f of 0.0023 and 0.16 respectively.[9–11] Their excited state fluorescence lifetimes (τ_f) are also at least one order of magnitude higher than that of the *para* analogues.[9–11] Thus, enhancement of Φ_f and τ_f could be achieved by structural modification. It has been shown that the extent of charge transfer is much higher for the *meta* analogues in comparison to the *para* analogues.[9,11] Thus, differential optical behaviour (w.r.t. Φ_f and τ_f values) has been shown for *meta* and *para* analogues.[9–12] This difference has been explained on the basis of the "*meta* effect" in analogy with the behaviour observed for stilbene derivatives.[10–18] Both for

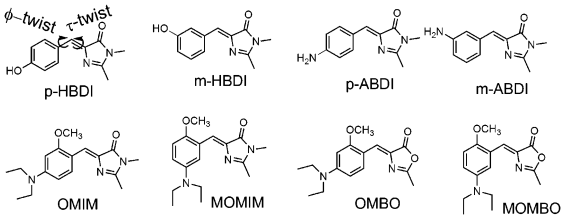

Chart 1 Chemical structures of the different GFP chromophore analogues.

Department of Chemical Sciences, Indian Institute of Science Education and Research (IISER), Mohanpur, Kolkata, West-Bengal, 741246, India.
E-mail: prasunchem@iiserkol.ac.in

† Electronic supplementary information (ESI) available: Experimental details, synthesis and characterization of GFP chromophore analogues, additional NMR data and stack plot, crystallographic table, additional steady state and time resolved spectroscopic data, *etc.* CCDC 1001355 and 1001357–1001359. For ESI and crystallographic data in CIF or other electronic format see DOI: 10.1039/c5cp03086b

para and *meta* analogues in aprotic solvents it has been shown that[9,11,12]

$$\Phi_f + 2\Phi_{ZE} = 1. \quad (1)$$

It has been reported that in aprotic solvents both for *para* and *meta* analogues *Z–E* isomerisation is the major nonradiative decay channel.[9–12] It has been reported that no other internal conversion plays any important role towards the non-radiative excited state decay channel.[9,11,12] It has also been shown for constrained GFP chromophore analogues where *Z–E* isomerisation is reduced that Φ_f is enhanced.[19–27] Thus, if the above eqn (1) holds true for unconstrained molecules, then, by structural modification, if the Φ_{ZE} value can be reduced then the Φ_f value can be enhanced. In order to probe the above idea we synthesized two sets of *para* and *meta* analogues namely OMIM, OMBO (*para* analogues) and MOMIM, MOMBO (*meta* analogues) (see Chart 1). In all these molecules we introduced a strong electron donating diethylamino group with the belief that the stronger electron donating effect will suppress the *Z–E* isomerisation and hence will improve the Φ_f value. To avoid perturbation from H-bonding all the molecules and the solvents explored here are without hydroxyl groups.

Results and discussion

The extent of charge transfer reflected in the magnitude of solvatochromic shift has been observed to be much higher in *meta* analogues (141 nm for MOMIM and 176 nm for MOMBO from hexane to ACN) (see Fig. 1 for MOMIM and ESI† for MOMBO) in comparison to their *para* analogues (OMIM (~30 nm) and OMBO (~30 nm)). Similar observations for other *meta* analogues have been reported in literature.[9,11] Also, Φ_f of MOMIM is much higher than OMIM. Moreover the fluorescence lifetime (τ_f) of the *meta* analogue MOMIM is ~1000 times higher (2.78 ns in ACN) than the *para* analogue OMIM (1.9 ps in ACN) (see Fig. 1). Similar observations have been observed for MOMBO and OMBO (see ESI†). Thus, it is confirmed that the enhanced extent of charge transfer is reflected in high values of both Φ_f and τ_f in *meta* analogues in comparison to *para* analogues.

As a next step it was necessary to calculate the Φ_{ZE} values of all four analogues in different solvents. Interestingly, unlike literature reports,[9,11] the *para* and *meta* analogues exhibit quite different Φ_{ZE} values (see Fig. 2, Table 1 and ESI†). The Φ_{ZE} values for the *para* analogues (OMIM, OMBO) are ~50%, however, the *meta* analogues (MOMIM and MOMBO) exhibit Φ_{ZE} values of ~10% or less in all solvents. No significant solvent dependence (from $CDCl_3$ to CD_3CN, to DMSO-d_6) was seen for either *para* or *meta* analogues. Thus, we can conclude that differential optical behaviour was observed between *para* and *meta* analogues (MOMIM and MOMBO) w.r.t. Φ_f, τ_f as well as Φ_{ZE} values.

Moreover, as can be seen from Table 1, eqn (1) holds good for *para* analogues but the equation fails completely for the studied *meta* GFP chromophore analogues. Thus, an apparent correlation between reduced Φ_{ZE} and enhanced Φ_f could be drawn for *meta* analogues. However, had *Z–E* isomerisation been the major nonradiative decay channel for *meta* GFP chromophore analogues, its very small value (<10%) would have increased the Φ_f value to be close to unity. But this was not the case as Φ_f for MOMIM was only 12% in hexane and 0.6% in ACN.

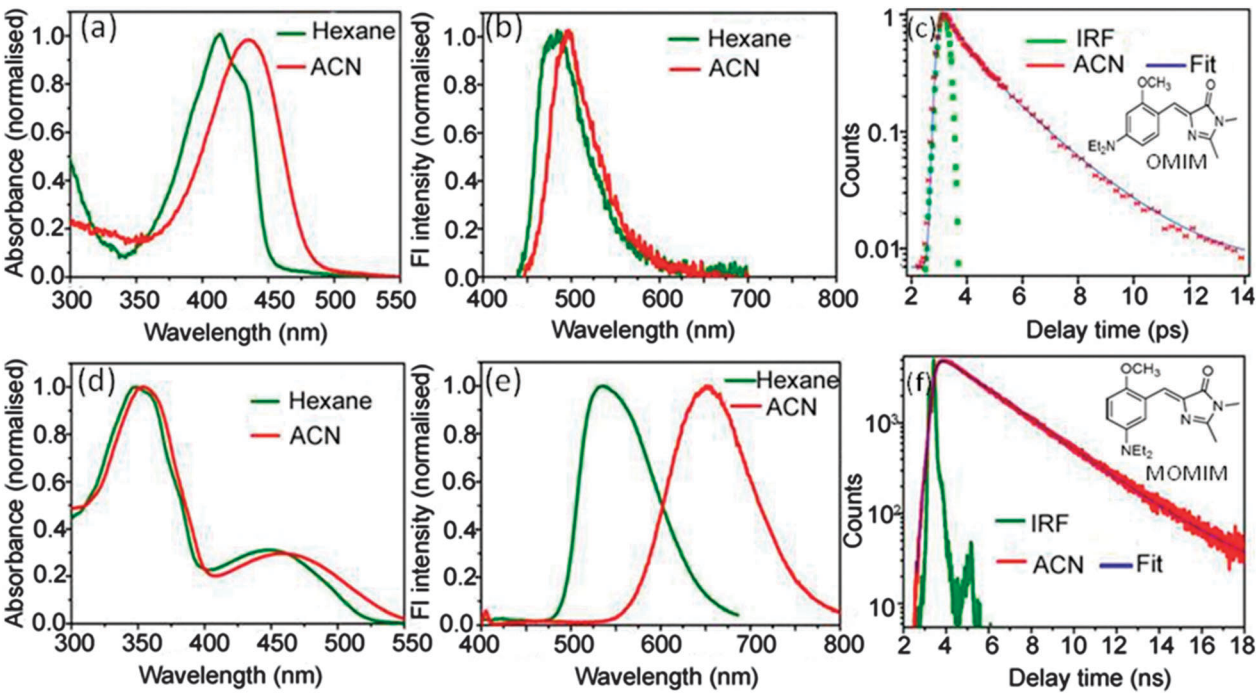

Fig. 1 Differential steady state (absorption (left), emission (middle) and time resolved (right)) fluorescence behaviour of OMIM (*para* analogue, above) and MOMIM (*meta* analogue, below).

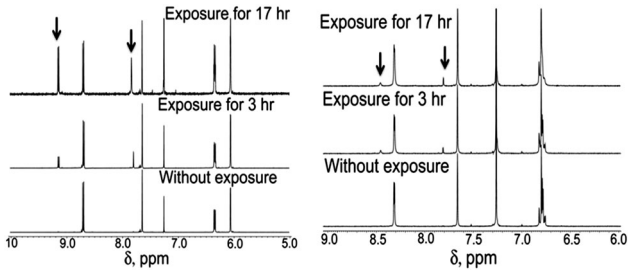

Fig. 2 Differential *Z*–*E* isomerisation for OMIM (*para* analogue, left) and MOMIM (*meta* analogue, right).

Table 1 Experimental parameters related to *Z*–*E* isomerisation

Compound	Solvent	% of *Z*-isomer[a]	% of *E*-isomer[b]	Φ_f	Φ_{ZE}	$\Phi_f + 2\Phi_{ZE}$
OMIM	$CDCl_3$	50	50	$<10^{-3}$	0.48	0.96
	CD_3CN	46	54	$<10^{-3}$	0.50	1.00
	DMSO-d_6	52	48	$<10^{-3}$	0.52	1.04
OMBO	$CDCl_3$	38	62	$<10^{-3}$	0.60	1.20
	CD_3CN	48	52	$<10^{-3}$	0.50	1.00
	DMSO-d_6	45	55	$<10^{-3}$	0.55	1.10
MOMIM	$CDCl_3$	NR	NR	**0.04**	**0.08**	**0.20**
	CD_3CN	NR	NR	**0.006**	**0.05**	**0.11**
	DMSO-d_6	NR	NR	**0.006**	**0.04**	**0.09**
MOMBO	$CDCl_3$	NR	NR	**0.02**	**0.13**	**0.28**
	CD_3CN	NR	NR	**0.002**	**0.04**	**0.09**
	DMSO-d_6	NR	NR	**0.002**	**0.06**	**0.13**

[a] At the photo-stationary state (PSS). [b] NR: PSS could not be reached even after 17 h indicating significantly slower kinetics for *meta* analogues in comparison to *para* analogues.

Thus, we can conclude that contrary to literature reports *Z*–*E* isomerisation is not the major nonradiative decay channel for these *meta* analogues. Thus it is necessary to know what kind of non-radiative decay is involved in the photophysics of these *meta* analogues.

In order to understand why eqn (1) fails completely for these *meta* GFP chromophore analogues and also to know what kind of major nonradiative decay could be taking place, we carried out structural analysis starting from ground state to excited state. We obtained single crystal X-ray structures of all four compounds. These crystal structures are depicted in Fig. 3. As can be seen from Fig. 3 all four compounds remain in a planar *Z* form with the –OMe group in the opposite direction to that of the imidazolidinone ring in the solid phase. As a next step, in order to know whether the same form persists in the solution phase, we carried out NMR measurements of all four compounds in different solvents. As can be seen from the NMR results (ESI†) even in the solution phase the ground state remains in the *Z* form. Thus, from single crystal X-ray and from NMR experiments we can conclude that the ground state structural form remains the same both in the solid and the solution phase for the *meta* analogues (and also for the *para* analogues). This means both *meta* and *para* analogues remain in same ground state structural form. Thus, we can make two important inferences: (i) that ground state structural heterogeneity does not exist; and (ii) that the differential optical behaviour is not due to ground state structural differences.

Ground state structural analysis could not provide significant clue regarding differential Φ_{ZE} values for *para* ($\sim$50%) and *meta* analogues ($<$10%). Moreover, it is also not understood, why instead of having very low Φ_{ZE} values, the *meta* analogues have much lower (than unity) Φ_f. First, we tried to understand the reason behind the differential magnitude of Φ_{ZE} values for *para* (50%) and *meta* ($<$10%) analogues. Our experimental observation was that the extent of charge transfer (in the planar configuration) in the *meta* analogues is much higher than that of the *para* analogues. Computational calculation results (see Fig. 4)

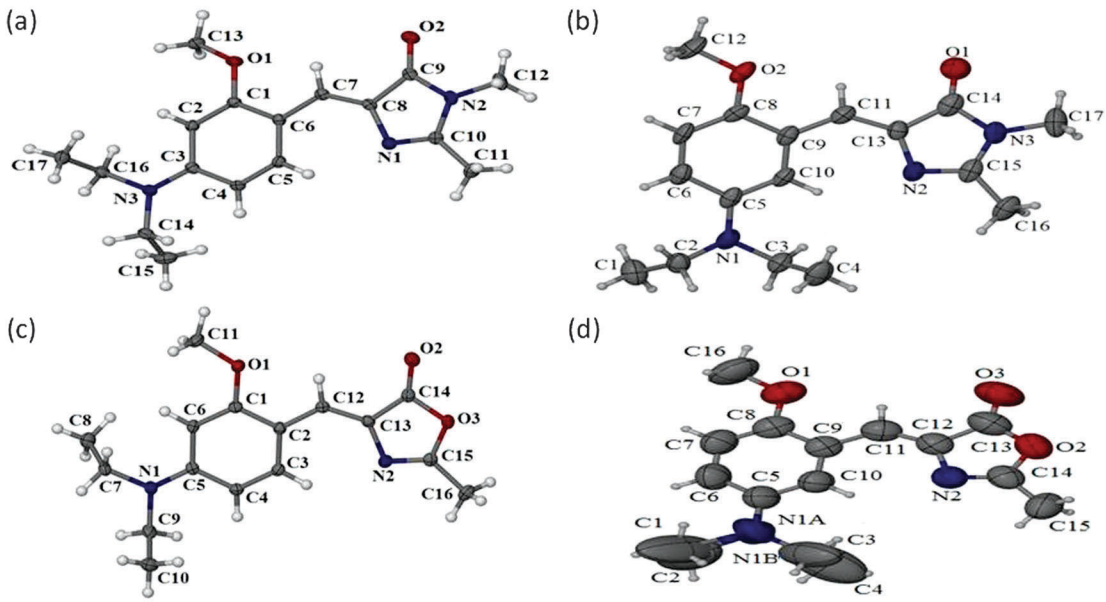

Fig. 3 Single crystal X-ray structure of OMIM (a), MOMIM (b), OMBO (c), MOMBO (d).

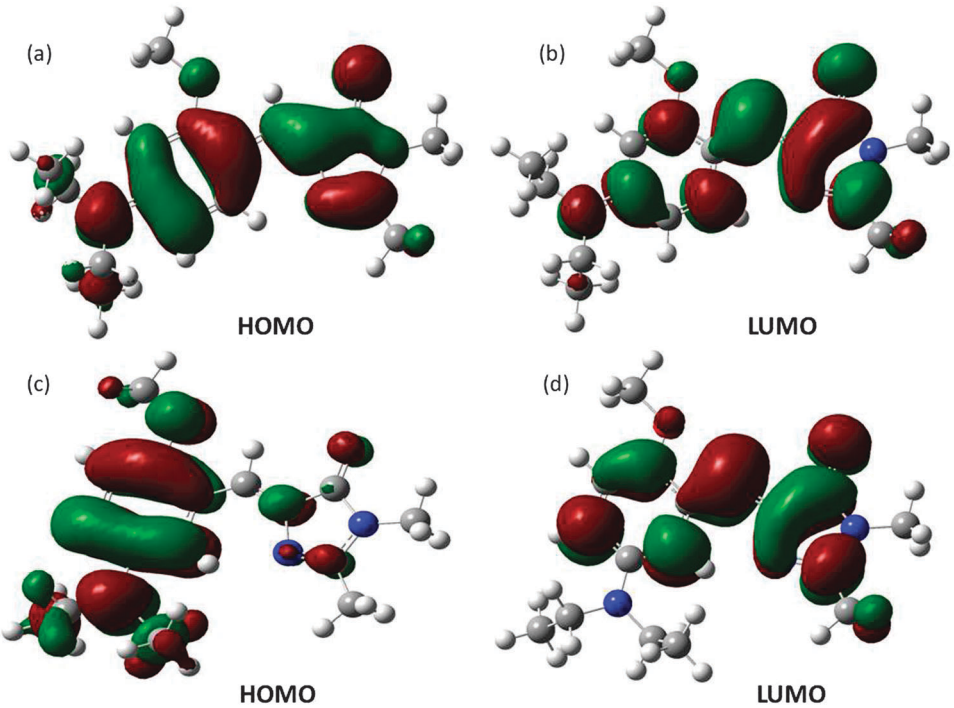

Fig. 4 Frontier molecular orbitals of OMIM (a and b) and MOMIM (c and d) calculated at the B3LYP/6-31G^{++} level.

show that on going from the HOMO to the LUMO the extent of charge separation is much higher for *meta* analogues than *para* analogues. Hence, the emission spectra of the *meta* analogues should show bigger solvatochromic shifts than those of the *para* analogues. This is exactly what we obtained experimentally. Thus, the computational calculations support the experimental results.

After initial photo-excitation from the ground state *Z* form to the FC excited state, the excited state species could either go to the planar ^{1}S* state or it could go to the τ-twisted ^{1}P* state. Which process will take place depends on the height of the (excited state) barrier between the planar and twisted state. Lowering the energy of the ^{1}P* twisted state relative to the planar ^{1}S* state decreases the barrier height and *vice versa*. Applying a similar analogy to that proposed by Michl and Bonačić-Koutecký for simple alkenes, the ^{1}P* state can be described as a combination of the biradical and charge transfer configuration.[14,28,29]

$$\psi_{^1P^*} = c_1\psi_{\text{biradical}(A^\bullet B^\bullet)} + c_2\psi_{CT(A^+B^-)} + c_3\psi_{CT(A^-B^+)}$$

An electron donating *para*-substituent group stabilizes the twisted state through resonance and thereby decreases the energy of the twisted ^{1}P* state.[14] In stark contrast, a *meta* electron donating group due to very weak mesomeric interaction cannot stabilize the twisted state (^{1}P*).[14]

The stabilization of the ^{1}S* state is much higher for *meta* analogues (as the polarity of the solvent increases), whereas according to the Michl and Bonačić-Koutecky model,[28,29] stabilisation of the ^{1}P* state is much higher for *para* analogues. Hence, for *meta* analogues the barrier height (from ^{1}S* to ^{1}P*) is much higher in comparison to *para* analogues (Scheme 1). Thus, *meta* analogues favour the planar rather than the twisted geometry in the excited state. This is why (solvatochromic) stabilisation of the planar ^{1}S* state is much higher for *meta* analogues. Moreover, because of the strong electron donating –NEt$_2$ group (in comparison to the –NH$_2$ group) the solvatochromic shift (from hexane to ACN) of MOMIM is much larger (142 nm) in comparison to *m*-ABDI (83 nm) (see ESI†).

We have estimated the magnitude of stabilization of the charge transferred planar singlet state (^{1}S*) of the *meta* analogues MOMIM and MOMBO to be 11.9 kcal mol^{-1} and 14.45 kcal mol^{-1} in comparison to that of *para* analogues (OMIM and OMBO respectively) from steady state emission in $CHCl_3$. The same for ^{1}P* state was not possible to calculate due to the non-fluorescent character of the state.

However, unlike *meta* analogues, for *para* analogues (Scheme 1a) the ^{1}P* state is energetically lower than the FC or ^{1}S* state. Thus, after initial excitation the molecule goes from the FC or ^{1}S* state to the ^{1}P* state for *para* analogues. Thus, the Φ_{ZE} value is much higher for *para* analogues (OMIM and OMBO) ($\Phi_{ZE} \sim 50\%$). From the ^{1}P* state the molecule relaxes to the ground electronic state in an ultrafast nonradiative fashion resulting in a much smaller Φ_f value ($\sim$0.0001) as well as τ_f value (femto–picosecond) for *para* analogues. Whereas for *meta* analogues, since the energy of the ^{1}P* state is comparable to the FC state or (much) higher than the ^{1}S* state, there is less probability that the *meta* analogues go from the ^{1}S* state to the ^{1}P* state. Hence, the Φ_{ZE} value is much reduced ($\Phi_{ZE} < 10\%$) for *meta* analogues (MOMIM and MOMBO). Thus, for *meta* analogues, molecule decays from ^{1}S* state, significantly radiatively resulting in much higher Φ_f value ($\sim$0.12 in hexane) as well as high τ_f value (5.22 ns in hexane).

Schemes somewhat similar to Scheme 1 have been reported previously.[9,11] However, that model can't explain the experimental

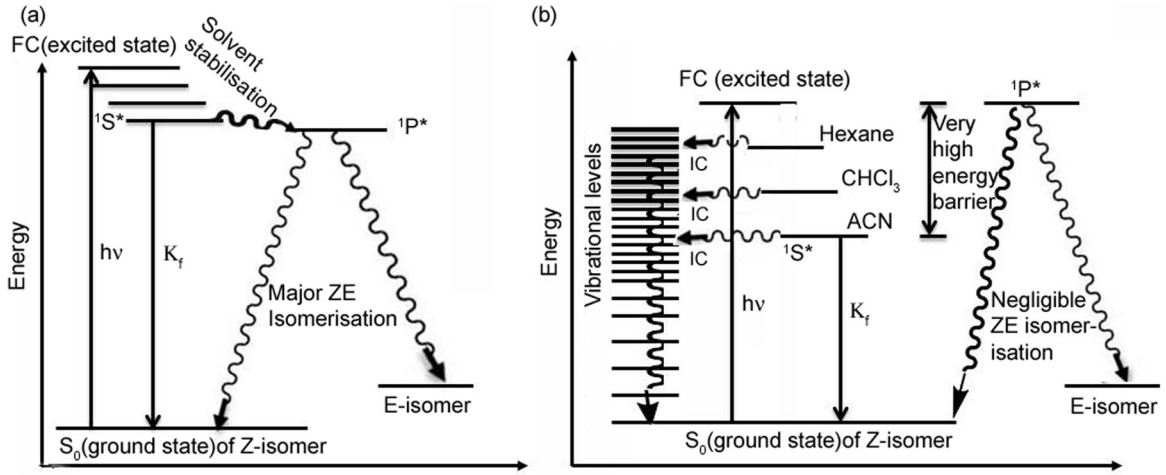

Scheme 1 Photophysical processes of (a) *para* analogues (OMIM and OMBO) and (b) *meta* analogues (MOMIM and MOMBO). (Drawn in accordance with the Perrin–Jablonski diagram shown in ref. 30.)

results we obtained. Moreover, though the twisted ^{1}P* state was conjectured to be much higher in energy than that of the planar ^{1}S* state in *m*-ABDI, still much higher *Z–E* isomerisation ($\Phi_{ZE} = 0.45$) in aprotic solvents has been reported.[11] As $\Phi_f + 2\Phi_{ZE} = 1$ holds for both *m*-ABDI and *p*-ABDI in aprotic solvents, it was concluded that *Z–E* isomerisation is the only nonradiative decay channel available to both *meta* and *para* compounds in spite of the slow isomerisation kinetics of the former.[9,11,12] Similar result was noted for *m*-HBDI by Tolbert *et al.* in nonaqueous solvents.[10]

Since the two sets of *para* and *meta* analogues exhibit widely different Φ_{ZE} values, quite contrary to previously reported results, *Z–E* isomerisation is not the major nonradiative decay channel for *meta* analogues in aprotic solvents and thus the reported models could not explain our experimental results. Thus, two different models need to be provided to understand the differential optical behaviour for *para* and *meta* analogues. These differential observations have been outlined in Scheme 1. From the scheme we could understand the electronic reason for such a reduced Φ_{ZE} value for *meta* analogues in comparison to the high Φ_{ZE} values for *para* analogues.

However, from $\Phi_f + 2\Phi_{ZE} = 1$, as the Φ_{ZE} value is $<10\%$, the Φ_f value should have been close to 80% for the *meta* analogues. But the experimental observation says that the Φ_f value is at best 12% (in hexane). This means there exists another non-radiative decay channel for *meta* analogues. Thus, it is necessary to know what kind of nonradiative decay channels could possibly be the reason for deviation of Φ_f from its near unity value for the *meta* analogues. Because of enhanced charge transfer, the emission maximum of MOMIM is considerably red shifted (547 nm in hexane and 688 nm in ACN) in comparison to the other *meta* analogues (*e.g.* *m*-ABDI has an emission maximum of 495 nm in hexane and 578 nm in ACN) reported in the literature.[9,11] The emission maxima of MOMIM and MOMBO are in the red whereas those for OMIM or OMBO as well as other reported *meta* analogues (*m*-HBDI and *m*-ABDI) are in the green region. Thus, the excited states of MOMIM and MOMBO are much more energetically stabilized in comparison to OMIM, OMBO and *m*-HBDI and *m*-ABDI. Thus, the energy difference between the stabilized excited state and the FC ground state is much smaller in case of MOMIM and MOMBO. Thus, following the energy gap law, nonradiative emission *i.e.* internal conversion from the stabilized excited state to the FC ground state becomes highly significant in the cases of MOMIM and MOMBO.[31–35]

However, the same is not so significant for *para* analogues or other *meta* analogues like *m*-ABDI.[9,11,12] Thus, because of the facile energy gap law governed internal conversion, which is a non-radiative decay process, the Φ_f value deviates greatly from the expected 80% value. As the polarity of the solvent increases the energy gap between the stabilized/solvated excited state and ground state decreases and hence the nonradiative internal conversion becomes more facile. This also explains why Φ_f decreases with increasing polarity in the case of MOMIM (0.12 in hexane to 0.006 in ACN) and MOMBO (0.10 in hexane to 0.002 in ACN). On going from hexane to acetonitrile, the radiative decay rate constant ($K_f = \Phi_f/\tau_f$) decreases from 0.21×10^8 s^{-1} to 0.021×10^8 s^{-1} and the nonradiative decay rate constant ($K_{nr} = (1 - \Phi_f)/\tau_f$) increases from 1.74×10^8 s^{-1} to 3.57×10^8 s^{-1}, respectively, for MOMIM. Thus, the large extent of the charge transfer (strong '*meta* effect') induced barrier in twisting makes *Z–E* isomerisation a minor nonradiative decay pathway for MOMIM and MOMBO. Rather, it is the energy gap law governed facile internal conversion which becomes the major nonradiative decay pathway for MOMIM and MOMBO. This observation is in complete contrast to that of the *para* analogues and the reported *meta* analogues (*m*-ABDI and *m*-HBDI) for which *Z–E* isomerisation is the only major nonradiative decay channel and for which any other internal conversion has been reported to be not at all important in aprotic solvents.

Conclusions

In conclusion, we synthesized two sets of non-hydroxylic unconstrained *para* and *meta* GFP chromophore analogues which exhibited differential optical properties in aprotic solvents w.r.t. Φ_f,

Φ_{ZE}, and τ_f values. For the *meta* analogues because of the strong "*meta* effect" the extent of charge transfer was much greater in comparison to the *para* analogues. Φ_f, and τ_f values of the *meta* analogues are ~1000 times higher than those of the *para* analogues. Φ_{ZE} values for *para* analogues are ~50% and for *meta* analogues are <10%. The well accepted equation $\Phi_f + 2\Phi_{ZE} = 1$ holds good for *para* analogues but fails completely for *meta* analogues. In contrast to existing literature reports, *Z*–*E* isomerization has been shown not to be the major nonradiative decay channel for *meta* analogues. Rather, because of enhanced charge transfer and hence a reduced energy gap between the stabilised excited state and ground state, the energy gap law governed facile internal conversion was shown to be the major nonradiative decay channel for *meta* analogues. These observations for *meta* analogues are in stark contrast to the existing literature of unconstrained non-hydroxylic GFP chromophore analogues. Two models have been provided which successfully explain the differential optical behaviour of *para* and *meta* GFP chromophore analogues. Thus, by structural variation the extent of charge transfer can be modulated and thus the nature of optical behaviour as well as the pathway of nonradiative excited state decay could be controlled.

Experimental details

Calculation of *Z*–*E* isomerisation efficiency

To measure the *Z*–*E* isomerisation quantum yield (Φ_{ZE}), solutions of low (mM) concentration range were used and irradiated with 370 nm light (8 W mercury lamp) without applying any special filter. The irradiation was followed by ^{1}H NMR at different time intervals. Since distinctive ^{1}H NMR signals are obtained for *Z* and *E* isomers, integration of the NMR peak corresponding to each isomer allowed us to know the isomer ratio at a certain time of irradiation. *p*-HBDI served as the reference standard (Φ_{ZE} = 0.48 in ACN).[9] The isomerisation quantum yield was calculated with the following equation:[9,36]

$$\frac{C_r \times V_r \times P_r}{\Phi_{ZEr} \times t_r} = \frac{C_s \times V_s \times P_s}{\Phi_{ZEs} \times t_s}$$

where *C* is the concentration of the substrate, *P* is the amount (%) of the initial *Z*-isomer that undergoes conversion to the *E*-isomer after irradiation, *V* is the volume of the solution, *t* is the irradiation time, and the subscripts r and s stand for the reference standard (*p*-HBDI) and the substrate (OMIM, OMBO, MOMIM and MOMBO) respectively. *P* was determined from the integrated intensity of the ^{1}H NMR peak for the *E*-isomer. The sample of ~10^{-3} M concentration was prepared in an NMR tube (Sigma Aldrich) and kept in a UV chamber for irradiation with a 370 nm light source. The back isomerisation in the ground state was also monitored by NMR. It was observed that back isomerisation after exposure was possible in the presence of light for OMIM and OMBO but not for MOMIM or MOMBO. However, in the dark the ground state back isomerisation from the *E*-isomer to the initial *Z*-isomer did not happen over a duration of three days for either of the derivatives. So, to keep ground state back isomerisation out of the calculation of Φ_{ZE}, the NMR tube was wrapped with aluminium foil after removal from the irradiation chamber. For the Φ_{ZE} value calculation, the sample was irradiated for a short time so that the irradiated sample containing a mixture of *E* and *Z* isomers was far from reaching a photo-stationary state (PSS).

Abbreviations used

Acronyms like *p*-HBDI, *m*-HBDI, *p*-ABDI, *m*-ABDI have previously been used in the literature.[9,10]

GFP	green fluorescence protein
OMIM	*o*-methoxy imidazolidinone
OMBO	*o*-methoxybenzoxazolidinone
MOMIM	*meta* diethylamino *o*-methoxy imidazolidinone
MOMBO	*meta* diethylamino *o*-methoxy benzoxazolidinone

Conflicts of interest

The authors declare no competing financial interests.

Acknowledgements

PKM thanks IISER-Kolkata for financial help and instrumental facilities. Support from the Fast-Track Project (SR/FT/CS-52/2011) of DST-India is gratefully acknowledged. PKM acknowledges Prof. P. Ramamurthy (NCUFP) for his help in femtosecond decay measurements. TC, and PPB thank CSIR, MM and VG thank IISER-Kolkata for their respective Fellowship.

References

1 W. Weber, V. Helms, J. A. McCammon and P. W. Langhoff, *Proc. Natl. Acad. Sci. U. S. A.*, 1999, **96**, 6177–6182.
2 A. Follenius-Wund, M. Bourotte, M. Schmitt, F. Iyice, H. Lami, J. J. Bourguignon, J. Haiech and C. Pigault, *Biophys. J.*, 2003, **85**, 1839–1850.
3 M. E. Martin, F. Negri and M. Olivucci, *J. Am. Chem. Soc.*, 2004, **126**, 5452–5464.
4 P. Altoe, F. Bernardi, M. Garavelli, G. Orlandi and F. Negri, *J. Am. Chem. Soc.*, 2005, **127**, 3952–3963.
5 S. Olsen and S. C. Smith, *J. Am. Chem. Soc.*, 2007, **129**, 2054–2065.
6 S. A. Olsen, *J. Chem. Theory Comput.*, 2010, **6**, 1089–1103.
7 G. J. Huang and J. S. Yang, *Chem. – Asian J.*, 2010, **5**, 2075–2085.
8 A. Baldridge, S. R. Samanta, N. Jayaraj, V. Ramamurthy and L. M. Tolbert, *J. Am. Chem. Soc.*, 2010, **132**, 1498–1499.
9 J.-S. Yang, G.-J. Huang, Y.-H. Liu and S.-M. Peng, *Chem. Commun.*, 2008, 1344–1346.
10 J. Dong, K. M. Solntsev, O. Poizat and L. M. Tolbert, *J. Am. Chem. Soc.*, 2007, **129**, 10084–10085.
11 C. W. Cheng, G. J. Huang, H. Y. Hsu, C. Prabhakar, Y. P. Lee, E. W. G. Diau and J. S. Yang, *J. Phys. Chem. B*, 2013, **117**, 2705–2716.
12 G. J. Huang, J. H. Ho, C. Prabhakar, Y. H. Liu, S. M. Peng and J. S. Yang, *Org. Lett.*, 2012, **14**, 5034–5037.

13 E. M. Crompton and F. D. Lewis, *Photochem. Photobiol. Sci.*, 2004, **3**, 660–668.
14 F. D. Lewis, S. R. Kalgutkar and J. S. Yang, *J. Am. Chem. Soc.*, 1999, **121**, 12045–12053.
15 H. K. Sinha and K. Yates, *J. Am. Chem. Soc.*, 1991, **113**, 6062–6067.
16 H. E. Zimmerman, *J. Am. Chem. Soc.*, 1995, **117**, 8988–8991.
17 H. E. Zimmerman, *J. Phys. Chem. A*, 1998, **102**, 5616–5621.
18 K. M. Solntsev, O. Poizat, J. Dong, J. Rehault, Y. Lou, C. Burda and L. M. Tolbert, *J. Phys. Chem. B*, 2008, **112**, 2700–2711.
19 L. Wu and K. Burgess, *J. Am. Chem. Soc.*, 2008, **130**, 4089–4096.
20 A. Baldridge, K. M. Solntsev, C. Song, T. Tanioka, J. Kowalik, K. Hardcastle and L. M. Tolbert, *Chem. Commun.*, 2010, **46**, 5686–5688.
21 M. S. Baranov, K. A. Lukyanov, A. O. Borissova, J. Shamir, D. Kosenkov, L. V. Slipchenko, L. M. Tolbert, I. V. Yampolsky and K. M. Solntsev, *J. Am. Chem. Soc.*, 2012, **134**, 6025–6032.
22 C. C. Hsieh, P. T. Chou, C. W. Shih, W. T. Chuang, M. W. Chung, J. Lee and T. Joo, *J. Am. Chem. Soc.*, 2011, **133**, 2932–2943.
23 K. P. Kent and S. G. Boxer, *J. Am. Chem. Soc.*, 2011, **133**, 4046–4052.
24 K. Do and S. G. Boxer, *J. Am. Chem. Soc.*, 2011, **133**, 18078–18081.
25 A. Baldridge, S. Feng, Y. T. Chang and L. M. Tolbert, *ACS Comb. Sci.*, 2011, **13**, 214–217.
26 J. S. Paige, K. Y. Wu and S. R. Jaffrey, *Science*, 2011, **333**, 642–646.
27 T. Chatterjee, D. Roy, A. Das, A. Ghosh, P. P. Bag and P. K. Mandal, *RSC Adv.*, 2013, **3**, 24021–24024.
28 V. Bonačić-Koutecký, J. Köhler and J. Michl, *Chem. Phys. Lett.*, 1984, **104**, 440–443.
29 V. Bonačić-Koutecký and J. Michl, *J. Am. Chem. Soc.*, 1985, **107**, 1765–1766.
30 B. Valeur, *Molecular Fluorescence – Principles and Applications*, WILEY-VCH Verlag GmbH, Weinheim, 2002.
31 N. J. Turro, V. Ramamurthy and J. C. Scaiano, *Modern molecular photochemistry of organic molecules*, University Science Books, Sausalito, CA, 2010.
32 R. Englman and J. Jortner, *Mol. Phys.*, 1970, **18**, 145–164.
33 C. Liu, K. C. Tang, H. Zhang, H. A. Pan, J. Hua, B. Li and P. T. Chou, *J. Phys. Chem. A*, 2012, **116**, 12339–16345.
34 J. V. Caspar and T. J. Meyer, *J. Phys. Chem.*, 1983, **87**, 952–957.
35 M. Bixon and J. Jortner, *J. Phys. Chem.*, 1994, **98**, 1289–1294.
36 G. J. Huang, C. W. Cheng, H. Y. Hsu, C. Prabhakar, Y. P. Lee, G. E. W. Diau and J. S. Yang, *J. Phys. Chem. B*, 2013, **117**, 2695–2704.